Wang *et al. Chem Synth* 2024;4:40
DOI: 10.20517/cs.2024.28

Chemical Synthesis

Research Article

Open Access

Check for updates

Post-modified porous aromatic frameworks for carbon dioxide capture

Zihao Wang, Yina Zhang, Li Jiang, Qiance Han, Qihaoyue Wang, Jiangtao Jia*, Guangshan Zhu*

Key Laboratory of Polyoxometalate and Reticular Material Chemistry of Ministry of Education, Faculty of Chemistry, Northeast Normal University, Changchun 130024, Jilin, China.

***Correspondence to:** Prof. Jiangtao Jia, Prof. Guangshan Zhu, Key Laboratory of Polyoxometalate and Reticular Material Chemistry of Ministry of Education, Faculty of Chemistry, Northeast Normal University, 5268 Renmin Street, Changchun 130024, Jilin, China. E-mail: jiangtaojia@nenu.edu.cn; zhugs100@nenu.edu.cn

How to cite this article: Wang Z, Zhang Y, Jiang L, Han Q, Wang Q, Jia J, Zhu G. Post-modified porous aromatic frameworks for carbon dioxide capture. *Chem Synth* 2024;4:40. https://dx.doi.org/10.20517/cs.2024.28

Received: 29 Feb 2024 **First Decision:** 20 May 2024 **Revised:** 27 May 2024 **Accepted:** 4 Jun 2024 **Published:** 8 Jul 2024

Academic Editor: Xiang-Dong Yao **Copy Editor:** Pei-Yun Wang **Production Editor:** Pei-Yun Wang

Abstract

A new method was developed for post-modification of porous aromatic framework-1 (PAF-1) with chloride and then amine groups confirmed by different characterizations such as nuclear magnetic resonance (NMR), X-ray photoelectron spectroscopy (XPS), and Fourier transform infrared spectroscopy (FTIR). Compared to PAF-1, the amine-functionalized PAF-1 (PAF-1-NH_2) exhibits a 50% improvement in carbon dioxide (CO_2) adsorption capacity reaching 42 $cm^3 \cdot g^{-1}$ at room temperature and 1 bar, and the uptakes under CO_2 concentration in air (4 kPa) and flue gas (150 kPa) also greatly increase. The column breakthrough experiments showed that PAF-1-NH_2 can separate CO_2 from a simulated flue gas of CO_2/N_2 (15:85, v/v) indicating its potential applications in post-combustion systems.

Keywords: Post-synthesis, porous frameworks, carbon dioxide capture, PAF-1

INTRODUCTION

It has been an international consensus that global warming threatens the sustainable development of human society. The main means to retard the trend is by reducing carbon dioxide (CO_2) concentration in the atmosphere[1]. A lot of global authorities have set CO_2 emissions reduction plans, and the Chinese government has set the goals of carbon peaking by 2030 and carbon neutrality by 2060. To realize these

goals, CO_2 capture and sequestration technologies are urgently needed. According to the literature, more than 80% of the CO_2 emission comes from the combustion of fossil fuels, and 60% originates from the coal and natural gas-fired power plants[2]. Currently, aqueous amine solutions are mainly used as the adsorbents for CO_2 capture in the industry; however, this process suffers from strong equipment corrosion, high regeneration energy input and evaporation pollution/loss of the liquid amines[3].

Gas capture techniques may address excess CO_2 emissions. For large-scale use industries, CO_2 capture methods include amine scrubbing, calcium cycling from post-combustion, and direct air capture[4]. Amine scrubbing has a higher adsorption capacity, but the loss of adsorption capacity during cycling is greater and more energy is usually required to desorb CO_2 due to its higher enthalpy of adsorption. Also, calcium cycling is widely used but faces high extra energy input[5]. Porous materials can overcome the problem of amine scrubbing and calcium cycling, with low energy input and high capacity[6]. At the present stage, research on first-generation capture technologies in China has made significant progress. The physical adsorption method has been successfully and commercially available in 2021[7].

Metal–organic frameworks (MOFs)[8-10] and porous organic frameworks (POFs)[11,12] have been found effective in CO_2 capture. The large surface area of porous materials provides various adsorption sites, facilitating effective interaction with CO_2 molecules. Furthermore, the reversible adsorption/desorption properties of porous materials allow for multiple cycles of use. Their unique structure and renewable characteristics offer an effective carbon capture and storage (CCS) adsorbent to address challenges associated with greenhouse gas emissions and the climate crisis[13]. Thus, MOFs and POFs are considered alternatives to replace the current liquid amine adsorbents.

Compared with relatively weak coordinate bond-connected MOFs, POFs are combined by stable covalent bonds with improved chemical stability making them available candidates for CO_2 capture under harsh conditions[14]. Porous aromatic framework-1 (PAF-1), a star material among the POFs, has an ultra-high Brunauer–Emmett–Teller (BET) surface area and stable structural properties[12]. Thanks to the high chemical stability, different functional groups have been decorated on the PAF-1 and gifting PAF-1 extra properties such as gas storage, separation, uranium capture, and so on[10]. As we know, phenylchloride, which has the potential to be converted to other different functional groups, has yet to be modified in PAF-1. Herein, we developed a previously unreported method to first post-modify phenylchloride groups and then convert them to amine groups on the skeleton of PAF-1, which shows impressive CO_2 capture properties. Various approaches were applied to demonstrate the success of the post-modifications, and our research could provide a new way for PAF chlorination and amine functionalization.

EXPERIMENTAL

Materials

All starting materials and solvents, unless otherwise specified, were obtained from Innochem Co. and used without further purification. Tetra(4-bromophenyl)methane (99%) was purchased from Jilin Chinese Academy of Sciences - Yanshen Technology Co., Ltd., and $AlCl_3$ (99+%) was provided by Aladdin.

Synthesis method

Synthesis of PAF-1

Synthesis of PAF-1 as reported[12]: In a glovebox, 1,5-cyclooctadiene (cod, 0.67 mL, 5.3 mmol), bis(1,5-cyclooctadiene)nickel(0) [$Ni(cod)_2$, 1.44 g, 5.2 mmol], 2,2'-bipyridine (2,2'-Bpy, 0.81 g, 5.2 mmol), and anhydrous N,N'-dimethylformamide (DMF) (76 mL) were added to a 250 mL double-neck flask. In another double-neck flask, a solution of tetra(4-bromophenyl)methane (0.63 g, 1 mmol) in DMF (19 mL) was

prepared. Both flasks were activated simultaneously at 80 °C for one hour. The activated monomer solution was then slowly transferred into the activated catalyst flask using a syringe. The reaction proceeded at 80 °C for 48 h. After cooling to room temperature, 6 M hydrochloric acid was added, and the solution was stirred for one hour until it turned green with a snowflake-like solid formation. The mixture was filtered, and the white solid obtained was thoroughly washed with water, methanol, and chloroform. The resulting white powder was dried under vacuum at 120 °C to yield a white powder (230 mg, 78% yield).

Synthesis of PAF-1-Cl

The introduction of chlorine into the framework draws on the method of insoluble molecular chlorination[15].

Under an argon atmosphere, PAF-1 (200 mg), $AlCl_3$ (0.2 g, 1.5 mmol), ICl (9.7 g, 60 mmol), and 30 mL of CCl_4 were added to a 100 mL flask. The mixture was vigorously stirred and heated to 80 °C, and the reaction was allowed to proceed for two days. After quenching with 50 mL of methanol, the mixture was filtered, and the resulting solid was thoroughly washed with hydrochloric acid, water, methanol, and chloroform. After vacuum drying, a white-gray solid was obtained (277 mg, 96% yield).

Synthesis of PAF-1-CN

Under an inert atmosphere, PAF-1-Cl (60 mg), anhydrous cesium carbonate (1g, 3 mmol), 3-Mercaptopropiononitrile (88 mg, 1 mmol) in anhydrous DMF (5 mL) were heated in a 20 mL single-neck glass bottle at 100 °C for 48 h. After cooling to room temperature, the solid was collected and washed with water, methanol and acetone several times. After drying, 80 mg of light yellow powder with a 87% yield was obtained[16].

Synthesis of PAF-1-COOH

Under an inert atmosphere, PAF-1-Cl (60 mg), anhydrous cesium carbonate (1g, 3 mmol), and thioglycolic acid (93 mg, 1 mmol) in anhydrous DMF (5 mL) were heated in a 20 mL single-neck glass bottle at 100 °C for 48 h. After cooling to room temperature, the solid was collected and washed with water, methanol and acetone several times. After drying, 86 mg of light yellow powder with a 91% yield was obtained[16].

Synthesis of PAF-1-OH

Under an inert atmosphere, PAF-1-Cl (60 mg), anhydrous cesium carbonate (1g, 3 mmol), and 3-Mercapto-1-propanol (93 mg, 1 mmol) in anhydrous DMF (5 mL) were heated in a 20 mL single-neck glass bottle at 100 °C for 48 h. After cooling to room temperature, the solid was collected and washed with water, methanol and acetone several times. After drying, 87 mg of light yellow powder with a 91% yield was obtained[16].

Synthesis of PAF-1-NH-Boc

Under an inert atmosphere, PAF-1-Cl (210 mg), anhydrous cesium carbonate (1g, 3 mmol), and 2-(Boc-amino)ethanethiol (53 mg, 3 mmol) in anhydrous DMF (5 mL) were heated in a 20 mL single-neck glass bottle at 100 °C for 48 h. After cooling to room temperature, the solid was collected and washed with water, methanol and acetone several times. After drying, 336 mg of light yellow powder with a 77% yield was obtained[16].

Synthesis of PAF-1-NH_2

Add PAF-1-NH-Boc (230 mg) into a single-neck flask containing 10 mL of concentrated hydrochloric acid and 10 mL of ethyl acetate under an inert gas atmosphere. Stir and heat to reflux for 48 h. Afterward, filter,

collect the solid, and thoroughly wash it with water, methanol, and acetone. Subsequently, the collected solid was added into a methanol solution containing 10 wt% sodium hydroxide and vigorously stirred at room temperature for 24 h. Filter and collect the solid, rinse thoroughly with water, and then subject it to Soxhlet extraction using methanol and chloroform as the solvent, respectively, for 6 h each. After drying, 106.8 mg pale yellow solid powder with a 73% yield was obtained[16].

Materials and physical measurements

^{13}C solid nuclear magnetic resonance (NMR) spectra were attained using a Bruker Avance III model 400 MHz NMR spectrometer at a cross-polarization/magic angle spinning (CP/MAS) rate of 5 kHz. The X-ray photoelectron spectroscopy (XPS) spectra were collected in a KRATOS. Fourier transform infrared spectroscopy (FTIR) spectra were performed on a Nicolet IS50 Fourier transforms infrared spectrometer.

N_2 isotherms at 77 K and some other gas isotherms at different temperatures were acquired using an Autosorb absorptiometer (Quantachrome, iQ2). Thermogravimetric analysis (TGA) was performed with a TGA/DSC 1 STARe system at a heating rate of 5 °C/min under an air atmosphere.

Breakthrough experiments

Breakthrough experiments were performed on a mixSorb S (3P instrument), a dynamic gas breakthrough device. A 0.189 g sample of PAF-1-NH_2 was loaded onto a stainless-steel column (1 mL volume, 0.45 cm inner diameter). Heat it under a vacuum at 120 °C for 8 h to obtain an activated sample. A CO_2/N_2 (15:85, v/v) gas mixture was allowed to flow onto the column. Use a mass spectrometer (Master 400) to monitor the outflow gas from the column.

RESULTS AND DISCUSSION

First, a new method that introduced chlorine into a framework is demonstrated [Figure 1A]. The ^{13}C cross-polarization/magic angle spinning NMR (^{13}C CP/MAS NMR) spectrum and XPS analysis confirmed the successful introduction of chlorine elements onto the framework of PAF-1. The solid-state NMR spectrum peaks of PAF-1 were assigned according to the reported literature [Figure 1][12]. ^{13}C NMR spectra of PAF-1-Cl show that the carbon peaks have significant fusion and obvious shifts. Notably, the peak at 126 ppm corresponding to the carbon labeled d almost disappears, indicating chlorination on this atom. From the structure of PAF-1, atom d has the least steric hindrance during chlorination which coincides with the ^{13}C NMR spectra. This agreement strongly proves that PAF-1 was successfully chlorinated during this experiment. Additionally, the high-resolution C 1s XPS spectra of PAF-1 have only two peaks of C–C and C=C bonds, whereas, in the XPS energy spectrum of PAF-1-Cl, it can be clearly seen that the new C–Cl bond peaks appear between 286-287 eV[17]. The post-chlorination changes are even more pronounced when examining the chlorine energy spectral intervals of the two materials [Figure 1C and D]. Specifically, the XPS spectrum of PAF-1 lacks a discernible peak near 200 eV[17]. In contrast, the corresponding placement in the XPS spectrum of PAF-1-Cl prominently exhibits peaks associated with Cl $2p_{1/2}$ and $2p_{3/2}$. Notably, the ratio of integral areas of these peaks is 1:2, providing additional justification for the validity of these findings. Meanwhile, a tetraphenylmethane contains 25 carbon atoms, and if it is replaced by a chlorine atom at position d, the ratio of carbon atoms to chlorine atoms is 25:4 = 6.25. The ratio of carbon atoms to chlorine atoms given by XPS spectroscopy is 86.99:13.01 ≈ 6.68, which is also compatible with the theoretical value [Supplementary Figure 1].

In this study, different functional groups are modified by PAF-1-Cl; comprehensive validation of the successful progression of the entire process is evidenced through FTIR spectra. This research involved a series of functional modifications of PAF-1, including PAF-1-CN, PAF-1-COOH and PAF-1-OH

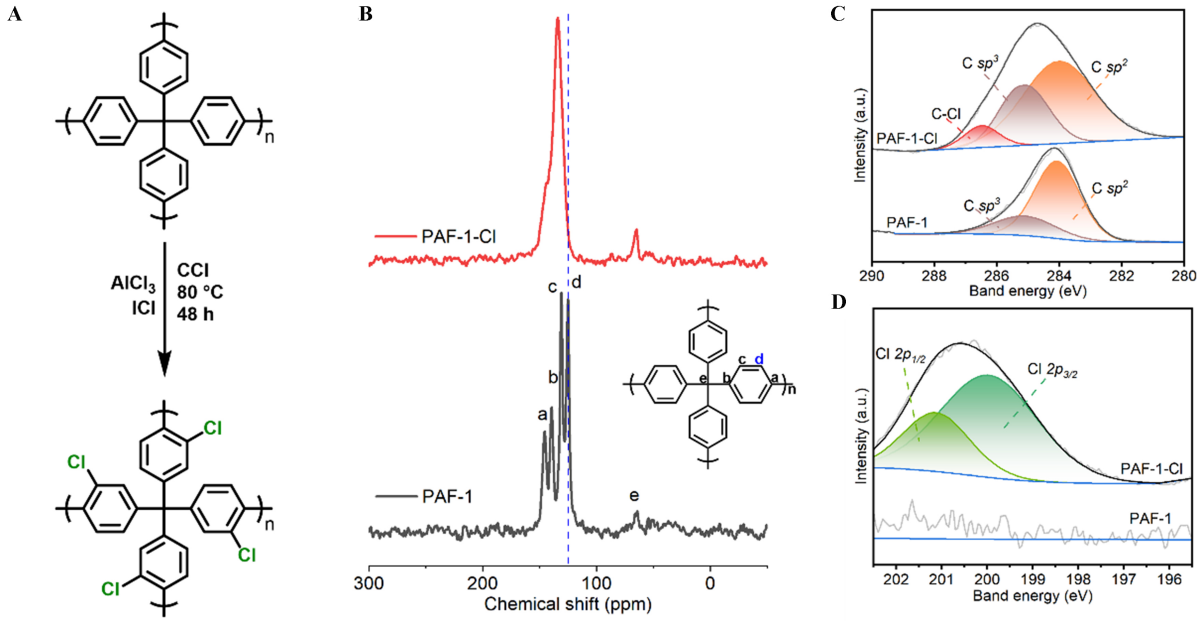

Figure 1. Schematic diagram of the post-modification process. (A) The new post-modified method for PAF-1; (B) ^{13}C CP/MAS NMR spectrum of PAF-1 and PAF-1-Cl; (C and D) XPS C *1s* and Cl *2p* spectrum of PAF-1 and PAF-1-Cl. PAF-1: Porous aromatic framework-1; CP/MAS: cross-polarization/magic angle spinning; NMR: nuclear magnetic resonance; XPS: X-ray photoelectron spectroscopy.

[Figure 2]. The characteristic vibrational peaks corresponding to these three materials are displayed in Supplementary Figures 2-4. Their physical adsorption characterizations are shown in Supplementary Figures 5 and 6. In order to solve the problem of CO_2 capture, we designed and synthesized post-modified PAF-1 containing amino groups that were commonly known in this application. As depicted in Figure 3A, PAF-1-Cl exhibits a distinctive new peak at 745 cm^{-1}, characteristic of C–Cl bonds, which diminishes in the next post-synthetic step where -Cl and subsequently engages in a continuous reaction with 2-(Boc-amino)ethanethiol. At the same time, PAF-1-NH-Boc displays new peaks at 1,721 and 1,170 cm^{-1}, which were assigned to the C=O and C–N stretch in the Boc group. After the deprotection, the resulting PAF-1-NH_2 shows the disappearance of the peaks at 1,721 and 1,170 cm^{-1}. Meanwhile, the -NH_2 peak shows at ~3,400 nm^{-1}, which is direct evidence of the successful modification of PAF-1-NH_2. Furthermore, the TGA results [Supplementary Figure 5] indicate that all these compounds showed high thermal stability. However, the weight of PAF-1-NH-Boc decreases by 22% at around 250 °C due to the decomposition of the Boc group[18]. This means that PAF-1-Cl contains one -NH-Boc group in each unit on average. Supplementary Figure 6 shows the scanning electron microscope (SEM) images with no marked change after modification. A transmission electron microscopy (TEM) image and the energy-dispersive X-ray spectroscopy (EDS) mapping images of PAF-1-NH_2 [Figure 3B-E] exhibited the uniform distribution of S and N elements, implying the success of the post-modification.

The N_2 and CO_2 adsorption isotherm of PAF-1-CN, PAF-1-COOH and PAF-1-OH were shown in Supplementary Figures 7 and 8. Apart from that, the N_2 sorption isotherm measurements were conducted on PAF-1, PAF-1-Cl, PAF-1-NH-Boc, and PAF-1-NH_2 at 77 K, revealing BET surface areas of 4,580, 1,077, 139, and 1,002 $m^2 \cdot g^{-1}$, respectively [Figure 4A and Supplementary Figure 9]. Simultaneously, the pore width decreases from 1.42 nm (PAF-1) to 1.08 nm (PAF-1-NH_2) [Supplementary Figure 10]. The nitrogen adsorption data and the change in the specific surface area suggest that the specific surface area of chlorinated PAF-1 decreases due to not only the larger chlorine atoms occupying the pores but also the

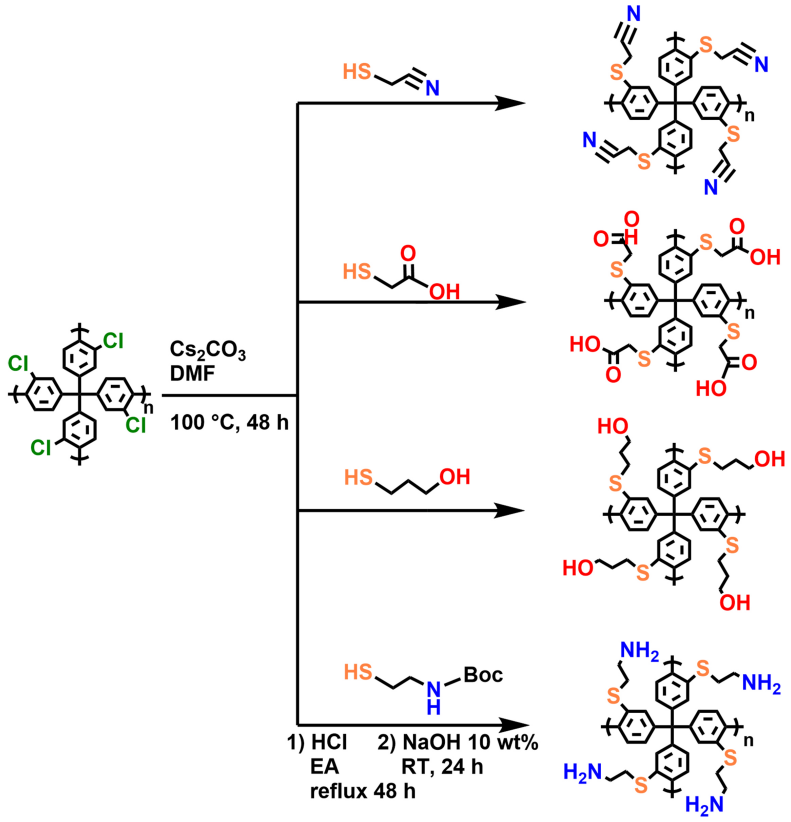

Figure 2. Different functional groups modified methods for PAF-1-Cl. PAF-1: Porous aromatic framework-1.

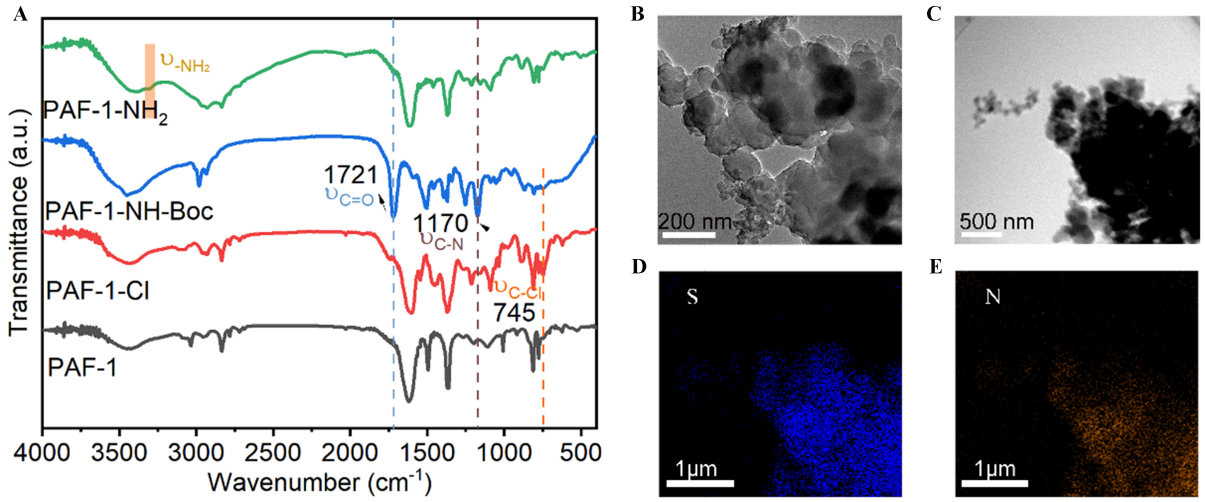

Figure 3. (A) FTIR spectra of PAF-1 (black), PAF-1-Cl (red), PAF-1-NH-Boc (blue) and PAF-1-NH_2 (green); (B) The TEM image of PAF-1-NH_2; (C-E) EDS maps of S, N and corresponding to (C). FTIR: Fourier transform infrared spectroscopy; PAF-1: porous aromatic framework-1; TEM: transmission electron microscopy; EDS: energy-dispersive X-ray spectroscopy.

increased weight of the chlorine atoms, leading to a drastic reduction in adsorption per unit mass (calculation details are in Supplementary Materials). Post-modification of amino groups with protecting Boc groups further decreases the specific surface area to about 100 $m^2 \cdot g^{-1}$, indicating nearly complete pore

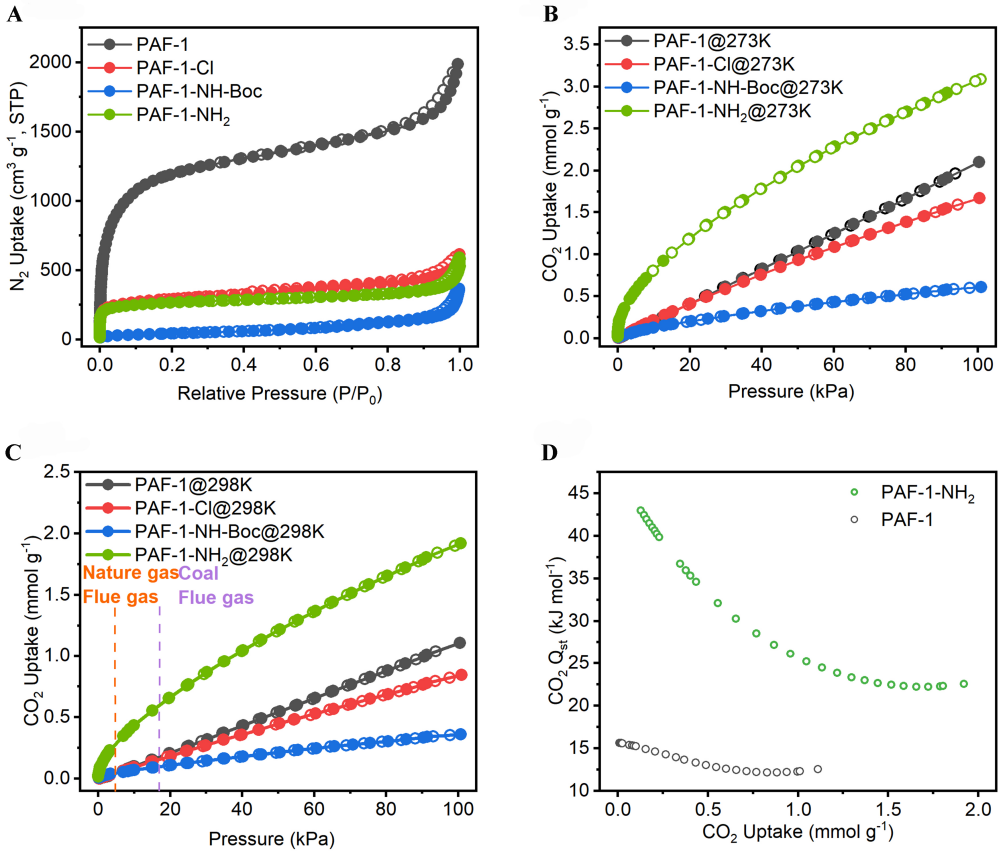

Figure 4. Gas absorption and desorption of PAF-1 and its derivations. (A) N_2 uptake at 77 K; (B) CO_2 uptake of PAF-1 and its derivations at 273 K; (C) CO_2 uptake of PAF-1 and its derivations at 298 K; (D) CO_2 Q_{st} of PAF-1 and PAF-1-NH_2. PAF-1: Porous aromatic framework-1.

blockage to nitrogen molecules due to the large molecular size of the Boc. This means that it is difficult for N_2 to enter the pores of PAF-1-NH-Boc. In this case, the BET surface area of PAF-1-NH-Boc is much less than that of PAF-1-Cl. Subsequent removal of the amino groups restores the specific surface area to about 1,000 $m^2 \cdot g^{-1}$, confirming the successful removal of protective groups and comparable specific surface area to PAF-1-Cl. These changes in specific surface area affirm the success of this post-modified PAF. Meanwhile, the N_2 adsorption capacities of PAF-1 and PAF-1-NH_2 at 273 and 298 K are shown in Supplementary Figure 12.

Figure 4B and C depicts the single-component CO_2 adsorption isotherms of PAF-1 and its modified derivatives. PAF-1 and PAF-1-Cl both have relatively low uptakes of 1.1 and 0.82 $mmol \cdot g^{-1}$ at 1 bar and 298 K, respectively. In comparison, PAF-1-NH-Boc exhibits lower CO_2 uptake across the entire experimental pressure range (0-100 kPa), attributed to pore blockage following post-modification. In contrast, the CO_2 sorption isotherm of PAF-1-NH_2 reveals a sharp increase in the adsorption branch at shallow CO_2 pressures (< 10 kPa), transitioning into a moderate slope between 10 and 100 kPa. Introducing dipolar and basic free amino groups provides preferential interactions with tetrapolar and acidic CO_2 molecules, thus enhancing the pro-CO_2 nature of PAF-1 after functionalization with amino groups[19].

Specifically, at 273 K, PAF-1-NH_2 exhibits a CO_2 adsorption capacity of 3.09 $mmol \cdot g^{-1}$, slightly decreasing to 1.91 mmol at 298 K. This represents a 50% enhancement in CO_2 adsorption compared to PAF-1.

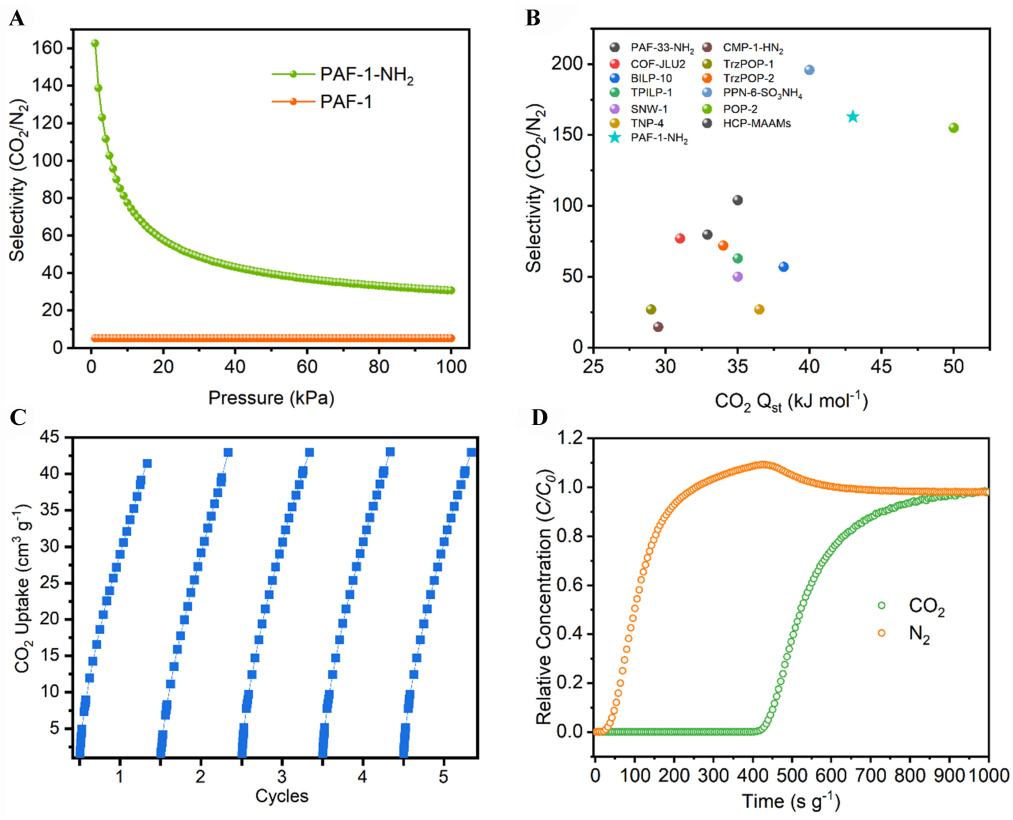

Figure 5. Separate ability of PAF-1-NH_2.(A) CO_2/N_2 selectivity of PAF-1 and PAF-1-NH_2; (B) CO_2/N_2 selectivity and CO_2 Q_{st} comparison with other POPs; (C) CO_2 cycles adsorption of PAF-1-NH_2; (D) Breakthrough curves of PAF-1-NH_2 for a CO_2/N_2 (15:85, v/v) gas mixture with a total flow of 10 mL·min^{-1} at 298 K and 1 bar. PAF-1: Porous aromatic framework-1; POPs: porous organic polymers.

Importantly, at 4 kPa (relevant to post-combustion capture from natural gas flue), 298 K[18], PAF-1-NH_2 demonstrates a substantial increase in CO_2 adsorption at 5.824 $cm^3 \cdot g^{-1}$ (0.26 mmol·g^{-1}), marking a 6.5-fold enhancement over PAF-1 (0.89 $cm^3 \cdot g^{-1}$, 0.04 mmol·g^{-1}). At 15 kPa (pertinent to post-combustion capture from coal flue gas)[20], PAF-1-NH_2 shows a significant increase in CO_2 uptake at 13.4 $cm^3 \cdot g^{-1}$ (0.6 mmol·g^{-1}), representing a 3.3-fold improvement compared to PAF-1 (3.98 $cm^3 \cdot g^{-1}$, 0.18 mmol·g^{-1}). These substantial enhancements in CO_2 uptake provide compelling evidence for the efficacy of incorporating aliphatic amines into PAFs, suggesting their promising potential as sorbents for efficient post-combustion CO_2 capture. Additionally, the CO_2 isothermal desorption curve for PAF-1-NH_2 exhibits no obvious hysteresis loop. The calculated CO_2 adsorption calorific values of PAF-1 and PAF-1-NH_2 are 16 and 44 kJ·mol^{-1}, respectively [Figure 4D][21]. This suggests that after adsorbing CO_2, PAF-1-NH_2 can easily desorb it, making the material convenient for CO_2 capture and recycling.

Based on the CO_2 and N_2 adsorption isotherms at 273 and 298 K of PAF-1 and PAF-1-NH_2, the CO_2/N_2 selectivity of porous materials could be calculated using the ideal adsorption solution theory (IAST) method. As shown in Figure 5A, The CO_2/N_2 selectivity of PAF-1 was only 5. With the addition of the amine, the selectivity of PAF-1-NH_2 for CO_2/N_2 was about 163, 33 times higher than that of the original material. Compared with other porous organic polymers in Figure 5B, PAF-1-NH_2 possesses a high enthalpy of CO_2 adsorption and an impressive separation selectivity [Supplementary Table 1]. The adsorption-desorption cycle of the material is critical for the use of industrial capture, and after five cycles, there was little change in CO_2 capacity [Figure 5C]. The results show that PAF-1-NH_2 is a promising

adsorptive separation material for CO_2 separation from industrial flue gas. To examine the practical separation potential of PAF-1-NH_2, the transient breakthrough experiments were conducted, in which a CO_2/N_2 (15:85, v/v) gas mixture flow over a fixed-bed column tightly filled with PAF-1-NH_2 samples by a flow of 10 mL·min^{-1} at 298 K and 1 bar. As shown in Figure 5D, N_2 elutes first without detectable CO_2, whereas CO_2 breaks out after a remarkably long retention time (412 s·g^{-1}), unveiling outstanding CO_2 separation performance at 298 K and 1 bar. The calculated CO_2 capture capacity based on a single breakthrough experiment is 0.461 mmol·g^{-1} in accord with the CO_2 isotherm.

CONCLUSIONS

We reported a new approach for functionalizing PAF materials, i.e., chloro-substituted PAF-1 and further converting to amino-functionalized PAF-1. XPS, ^{13}C NMR and FTIR confirm the successful post-modification of different groups such as -Cl and -NH_2. This method can also modify PAFs with various functional groups such as -SH and -CHO, thus adapting PAFs to various application scenarios. The CO_2 adsorption-desorption isotherms and CO_2/N_2 dynamic breakthrough of PAF-1-NH_2 were characterized, and we also observed that PAF-1-NH_2 owns excellent performance in CO_2 capture for dealing with post-combustion gases.

DECLARATIONS

Authors' contributions

Conception: Jia J, Zhu G
Planned the study, analyzed the data, and wrote the manuscript: Wang Z, Jia J
Synthesis and analytical discussions: Jiang L, Zhang Y
SEM and TEM characterization: Han Q, Wang Q

Availability of data and materials

Not applicable.

Financial support and sponsorship

The authors are grateful for financial support from the National Natural Science Foundation of China (Grant Nos. 22131004 and U21A20330) and the "111" project (No. B18012).

Conflicts of interest

Zhu G served as an editorial member of *Chemical Synthesis* but was not involved in the editorial process of the work, while the other authors have declared that they have no conflicts of interest.

Ethical approval and consent to participate

Not applicable.

Consent for publication

Not applicable.

REFERENCES

1. Yin Y, Kang X, Han B. Two-dimensional materials: synthesis and applications in the electro-reduction of carbon dioxide. *Chem Synth* 2022;2:19. DOI
2. Choi S, Drese JH, Jones CW. Adsorbent materials for carbon dioxide capture from large anthropogenic point sources. *ChemSusChem*

2009;2:796-854. DOI PubMed

3. Hack J, Maeda N, Meier DM. Review on CO_2 capture using amine-functionalized materials. *ACS Omega* 2022;7:39520-30. DOI PubMed PMC
4. Zhai R, Zhang L, Gu M, et al. A review of phosphorus structures as CO_2 reduction photocatalysts. *Small* 2023;19:e2207840. DOI PubMed
5. Hanifa M, Agarwal R, Sharma U, Thapliyal P, Singh L. A review on CO_2 capture and sequestration in the construction industry: emerging approaches and commercialised technologies. *J CO2 Util* 2023;67:102292. DOI
6. Abdelhamid HN. Removal of carbon dioxide using zeolitic imidazolate frameworks: adsorption and conversion via catalysis. *Appl Organomet Chem* 2022;36:e6753. DOI
7. Zhang X, Li Y, Ma Q, Liu L. Development of carbon capture, utilization and storage technology in china. *Chin J Eng Sci* 2021;23:70. DOI
8. Li H, Eddaoudi M, O'Keeffe M, Yaghi OM. Design and synthesis of an exceptionally stable and highly porous metal-organic framework. *Nature* 1999;402:276-9. DOI
9. Jiang L, Jia J, Ma Y, Tian Y, Zou X, Zhu G. Metal–carbon bond metal-organic frameworks with permanent porosity. *Chem* 2024;10:557-66. DOI
10. Jia J, Sun F, Fang Q, et al. A novel low density metal-organic framework with pcu topology by dendritic ligand. *Chem Commun* 2011;47:9167-9. DOI PubMed
11. Côté AP, Benin AI, Ockwig NW, O'Keeffe M, Matzger AJ, Yaghi OM. Porous, crystalline, covalent organic frameworks. *Science* 2005;310:1166-70. DOI PubMed
12. Ben T, Ren H, Ma S, et al. Targeted synthesis of a porous aromatic framework with high stability and exceptionally high surface area. *Angew Chem Int Ed Engl* 2009;48:9457-60. DOI PubMed
13. Siegelman RL, Kim EJ, Long JR. Porous materials for carbon dioxide separations. *Nat Mater* 2021;20:1060-72. DOI PubMed
14. Tian Y, Zhu G. Porous aromatic frameworks (PAFs). *Chem Rev* 2020;120:8934-86. DOI PubMed
15. Dong R, Pfeffermann M, Skidin D, et al. Persulfurated coronene: a new generation of "sulflower". *J Am Chem Soc* 2017;139:2168-71. DOI PubMed
16. Legru A, Verdirosa F, Hernandez JF, et al. 1,2,4-Triazole-3-thione compounds with a 4-ethyl alkyl/aryl sulfide substituent are broad-spectrum metallo-β-lactamase inhibitors with re-sensitization activity. *Eur J Med Chem* 2021;226:113873. DOI PubMed
17. Pełech I, Narkiewicz U, Moszyński D, Pełech R. Simultaneous purification and functionalization of carbon nanotubes using chlorination. *J Mater Res* 2012;27:2368-74. DOI
18. Han X, Zhou Z, Wang K, et al. Crystalline polyphenylene covalent organic frameworks. *J Am Chem Soc* 2024;146:89-94. DOI PubMed
19. Jiang W, Duan L, Qiao J, et al. Novel star-shaped host materials for highly efficient solution-processed phosphorescent organic light-emitting diodes. *J Mater Chem* 2010;20:6131. DOI
20. Raganati F, Miccio F, Ammendola P. Adsorption of carbon dioxide for post-combustion capture: a review. *Energy Fuels* 2021;35:12845-68. DOI
21. Ben T, Li Y, Zhu L, et al. Selective adsorption of carbon dioxide by carbonized porous aromatic framework (PAF). *Energy Environ Sci* 2012;5:8370. DOI